Journal of the European Ceramic Society 17 (1997) 1019–1026

PII: S0955-2219(96)00172-0
0955-2219/97/$17.00

Structural and Electrical Characterization of Titania-Doped YSZ

L. S. M. Traqueia,[a] T. Pagnier[b] & F. M. B. Marques[a,*]

[a]Ceramics and Glass Engineering Department, University of Aveiro, 3810 Aveiro, Portugal
[b]LEPMI-ENSEEG, BP 75, 38402 Saint Martin d'Hères, France

(Received 16 April 1996; accepted 19 August 1996)

Abstract

Solid solutions and composites based on YSZ (yttria-stabilized zirconia) with titania additions up to 20 mol% were prepared by solid state reaction. Structural characterization included XRD and Raman spectroscopy. Electroded samples were also studied by impedance spectroscopy in air between 573 and 1273 K. The ionic conductivity of these solid solutions decreases with increasing titania content. A sharp drop in conductivity is observed for specimens with compositions near to the usually assumed solubility limit of titania in the fluorite phase (about 10 mol%). This decrease is of almost one order of magnitude with respect to undoped or lightly doped samples. A smaller composition dependence is observed for higher titania additions (10–20 mol% TiO_2). Raman results show that tetragonal short range order is found in the cubic fluoritic phase well below the 10 mol% TiO_2 addition. This short range order is explained by the ability of Ti to achieve a sixfold oxygen coordination. As a consequence, a decrease in the concentration of mobile oxygen vacancies is expected, which is the reason for the electrical conductivity decrease.

1 Introduction

When zirconia is stabilized in the cubic structure by the addition of a lower valence cation, oxygen vacancies are also introduced in the anion sublattice to compensate for the charge of the dopant cation. Yttrium oxide is one of the best known dopants for zirconia and yttria-stabilized zirconia (YSZ) is presently the state-of-the-art electrolyte for high-temperature applications of oxygen ion conductors (e.g. oxygen sensors or fuel cells). The role of aliovalent dopant cations on the transport properties of zirconia-based solid solutions has been studied in detail for many years. It is usually accepted that these dopants interact with oxygen vacancies causing the formation of defect associates of dopant cations and oxygen vacancies. This type of approach can explain changes in activation energy of ionic conductivity with temperature, and with the charge and size of the dopant cation. Minimum defect association energies are found when the dopant cation has an ionic radius similar to that of the host cation.[1–2] Recent structural studies have shown that, depending on the size and valence of the dopant cation, oxygen vacancies might be preferentially located near the dopant or the host cation.[3–5]

The role of tetravalent dopants on the ionic conductivity of cubic zirconia-based solid solutions has received less attention until recently. ZrO_2–CeO_2–Y_2O_3 was one of the first systems studied in detail.[6–8] The experimental observation is that for small additions of ceria (10 mol%), a slight decrease in ionic conductivity is observed. For almost complete substitution of ceria for zirconia, the ionic conductivity increases and approaches the ionic conductivity of CeO_2–Y_2O_3 solid solutions. More recently, titania-doped YSZ has been given much attention because of potential applications of mixed conduction under reducing conditions.[9–20] The effect of titania additions to YSZ was found more pronounced than for identical ceria additions, resulting in a decrease in ionic conductivity in air of about one order of magnitude, for dopant levels approaching the usually assumed solubility limit in the cubic structure (about 10 mol% titania).

The most obvious differences between ceria and titania as dopants are the radius of the dopant cation and the structure of the corresponding oxides. Thus, the present work aims at a better understanding of the role of titania on the ionic

*To whom correspondence should be addressed.

transport properties of zirconia-based solid solutions, focusing on structural aspects. For this type of approach, XRD and Raman spectroscopy will be employed in order to evaluate the relative potential of both techniques in the identification of structural changes which might explain observed differences in electrical performance.

2 Experimental Procedure

Sintered discs of mixtures of titania and YSZ (8 mol% Y_2O_3, from Tosoh Co.) were prepared by high-temperature firing (1773 K, 4 h), after ball milling and pressing of powder mixtures. The titania dopant levels (x) used in this work were 1, 2, 3·5, 5, 10 and 20 mol%. The notation xTiYSZ will be used to describe these materials, where x corresponds to the titania content in the powder mixtures (xTiYSZ = (100 − x) mol% YSZ + x mol% TiO_2). SEM and EDS analysis were used to study the microstructure and composition of these materials. Samples were polished and thermally etched before microstructural observation.

XRD and Raman spectroscopy were used for structural characterization. Raman spectra were obtained with a Dilor XY multichannel spectrometer. A resolution of 3 cm^{-1} was chosen. The excitation line 514·53 nm (green) of an Ar-ion laser was used. Experiments were carried out in a backscattering geometry in micro Raman. A 50× objective was used with a spot diameter of 1·13 μm. All experiments were carried out with a laser power of 50 mW, the power finally reaching the sample being 6 mW. Spectra were taken between room temperature and 873 K.

Porous platinum electrodes were deposited on specimens for impedance measurements in air, performed with a HP 4284-A Precision LCR Meter (20 Hz–1 MHz), in the temperature range 573–1273 K.

3 Experimental Results

3.1 Structure and microstructure

3.1.1 XRD and SEM

Based on XRD and SEM observations, preliminary work on this system identified the solubility limit of titania in the fluorite phase in the order of 10–15 mol%, obviously depending on the exact Zr/Y proportions in YSZ.[9,11,14,21] In this work, for 10TiYSZ the diffractogram already shows some small peaks indicating the formation of a tetragonal phase, besides the fluorite phase. The presence of this second (tetragonal) phase has been already suggested in recent studies on similar compositions.[15,20] However, up to 5 mol% titania additions only the cubic phase could be identified by XRD (Fig. 1, lines (a)–(c)). Microstructural observations also suggest a single-phase material (Fig. 2(a)).

For high dopant levels (> 10 mol% TiO_2) SEM observations indicate that a third phase is clearly present (zirconium titanate). This is also supported by the monotonous decrease in the lattice parameter of the fluorite phase with increasing dopant content, up to about 10 mol% TiO_2. Above this value the lattice parameter becomes almost composition-independent. For the 10TiYSZ composition, traces of an apparently new phase could be noticed in samples fired at 1873 K, consisting of quite small grains located at grain boundaries of large grains. However, no positive identification of this phase has been performed.[19] In the present case, for samples fired at 1773 K, the grain boundaries were apparently clean (Fig. 2 (b)), identical to those already observed for firing temperatures of 1573 K.[19]

Lastly, for the 20TiYSZ samples, the formation of the titanate phase (usually identified as $ZrTiO_4$) is clear either by XRD (Fig. 1, line (e)) or SEM (Fig. 2 (c)). The exact composition of this titanate is still controversial. Apparently, the presence of Y_2O_3 has a stabilizing effect on $ZrTiO_4$ at low temperature, while in the absence of Y_2O_3, the stable phase becomes $ZrTi_2O_6$.[22] However, EDS analysis performed in this work on several grains of this zirconium titanate phase indicated a Zr/Ti atomic ratio of about 2 in all cases.

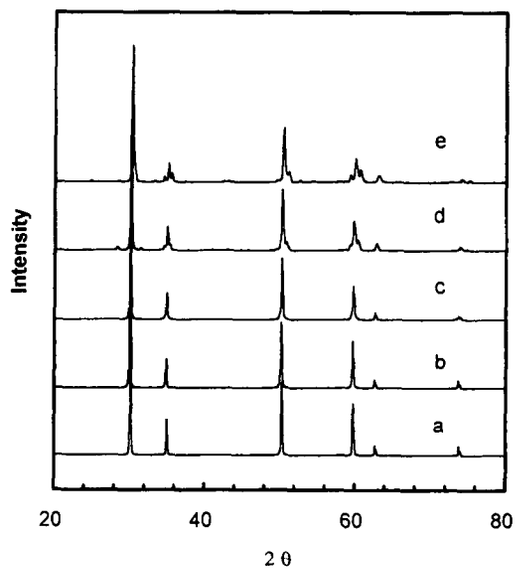

Fig. 1. XRD patterns of (a) 1TiYSZ, (b) 3·5TiYSZ, (c) 5TiYSZ, (d) 10TiYSZ and (e) 20TiYSZ. In (a)–(c) only the fluorite phase is found. The presence of a tetragonal phase can be noticed in (d), while the formation of a zirconium titanate is observed in (e).

(a)

(b)

(c)

Fig. 2. SEM microstructures of (a) 3·5TiYSZ, (b) 10TiYSZ and (c) 20TiYSZ, after polishing and thermal etching. The small white grains in (c) correspond to the zirconium titanate phase.

3.1.2 Raman spectroscopy

Figure 3 shows the room-temperature spectra of all the samples. The YSZ spectrum corresponds to the well-known spectrum of cubic zirconia.[23–27] In the fluoritic structure, a single vibration of symmetry F_{2g} is Raman active. However, the lack of long range order in the anion sublattice breaks the selection rules and the features observed between 0 and 800 cm^{-1} are assumed to be an image of the density of states. The broad peak appearing at 623 cm^{-1} is sometimes attributed to a F_{2g} vibration.[23] However, the zone centre F_{2g} mode is expected at about 450 cm^{-1} and this point merits a further analysis.

Titania additions below the usually assumed solid solution limit (i.e. for all samples except 20TiYSZ) give rise to new broad peaks located at 149, 261 (strong), 322, 462, 630 and 720 cm^{-1}. These new features cannot be attributed to either the rutile (bands at 447 and 612 cm^{-1}) or the anatase (very intense band at 144 cm^{-1}) structures of TiO_2. This result is consistent with the XRD results showing that Ti ions are in substitution for Zr ions, and therefore are coordinated to eight oxygens instead of six for TiO_2. On the contrary, the new bands fit well with the spectrum of tetragonal zirconia, except for the peak at 720 cm^{-1} which is not present in the Raman spectrum of tetragonal zirconia.

The Raman spectrum of xTiYSZ ($x \leq 10$) can be taken as the sum of a spectrum of cubic zirconia and that of tetragonal zirconia. This is more

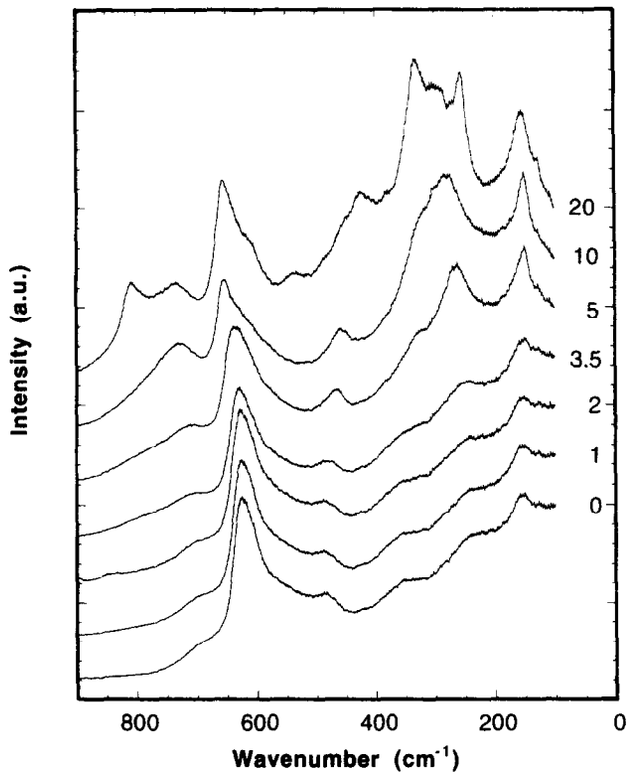

Fig. 3. Raman spectra of xTiYSZ samples at room temperature.

clearly shown in Fig. 4, where the spectrum of cubic zirconia has been subtracted from the experimental spectra of xTiYSZ. The amount of cubic zirconia spectrum to subtract has been manually adjusted so that the resulting spectrum does not present negative values and the results are only semi-quantitative. Nevertheless, the major peaks of tetragonal zirconia appear in the subtracted spectra. The band at 720 cm^{-1} also appears very nicely, even for low titania content, on the subtracted spectra. Its intensity is strongly correlated to the amount of titania dissolved into YSZ. The fraction of cubic zirconia spectrum which was subtracted from the spectra is shown as a function of the amount of titania in Fig. 5. This subtraction method seems to us better than that consisting in measuring peak ratios as proposed in Ref. 28.

The Raman spectra were also collected at different temperatures between room temperature and 873 K. A typical example is given in Fig. 6 ($x = 5$). The spectral changes are small. A broadening of the bands and a small decrease of their amplitudes are observed. This is a common phenomenon in Raman spectroscopy.

For the highest titania content (20TiYSZ), new bands appear. Subtraction of the 10TiYSZ spectrum from the 20TiYSZ one gives the spectrum shown in Fig. 7, which is comparable to the one published for $ZrTiO_4$.[29] A careful examination of the 10TiYSZ spectrum, especially in Fig. 4, shows that $ZrTiO_4$ is already present in this sample, as has been observed in SEM experiments. This could explain the apparent shift towards higher wavenumbers of the peaks located at 261, 640 and 720 cm^{-1} in the 5TiYSZ spectrum and at 280, 651 and 730 cm^{-1} in the 10TiYSZ spectrum and to the loss of details in the 250–400 cm^{-1} region of the 10TiYSZ spectrum.

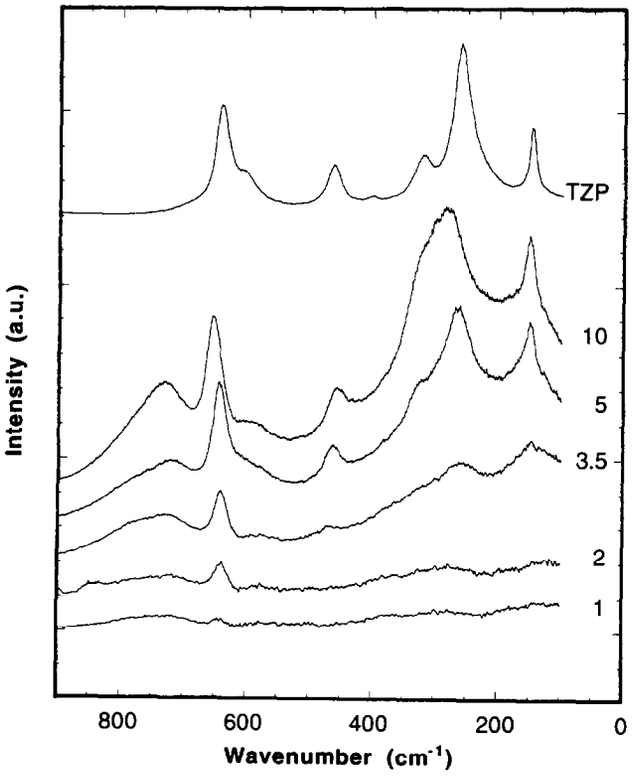

Fig. 4. Difference spectra obtained by subtracting YSZ Raman spectrum from the experimental Raman spectra of xTiYSZ ($1 \leq x \leq 10$). The Raman spectrum of a tetragonal polycrystalline zirconia (ZrO_2–3 mol% Y_2O_3 from Tosoh) is also shown for comparison and labelled TZP.

3.2 Electrical behavior

Typical impedance plots obtained in air for different titania-doped YSZ compositions (1, 3·5, and 20 mol% TiO_2), in the range 573–673 K, are shown in Fig. 8. The direct plot of the imaginary part of the complex impedance (Z") versus the real part (Z') has been changed to be able to show data obtained at three different temperatures within the same scale. The Z" and Z' values were divided by the maximum value of Z" at each temperature (Z" at the relaxation frequency for bulk grain behavior) yielding a non-dimensional and normalized impedance (Z_{normal}). In this manner, for a perfect RC behavior, the bulk arc (high frequency) should cross the real axis at the value 2. Values larger than 2 correspond to depressed arcs. This type of presentation also allows for a simple identification of the role of temperature on the relative magnitude of bulk and grain boundary arcs. The trend now observed corresponds to the classical one: because of a higher activation energy for ionic conduction at the grain boundaries than in the bulk, grain boundary arcs become less relevant with increasing temperature.

Data shown in Fig. 8 indicate that on increasing titania content, within the assumed solubility limit in the fluorite phase, a clear definition of the grain boundary arc is obtained. For titania contents exceeding 10 mol%, only one arc can be noticed,

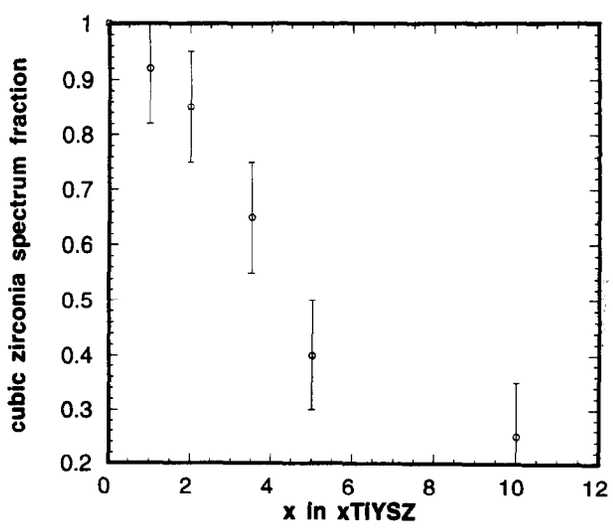

Fig. 5. Amount of cubic zirconia spectrum to subtract from experimental spectra to obtain the difference spectra of Fig. 4.

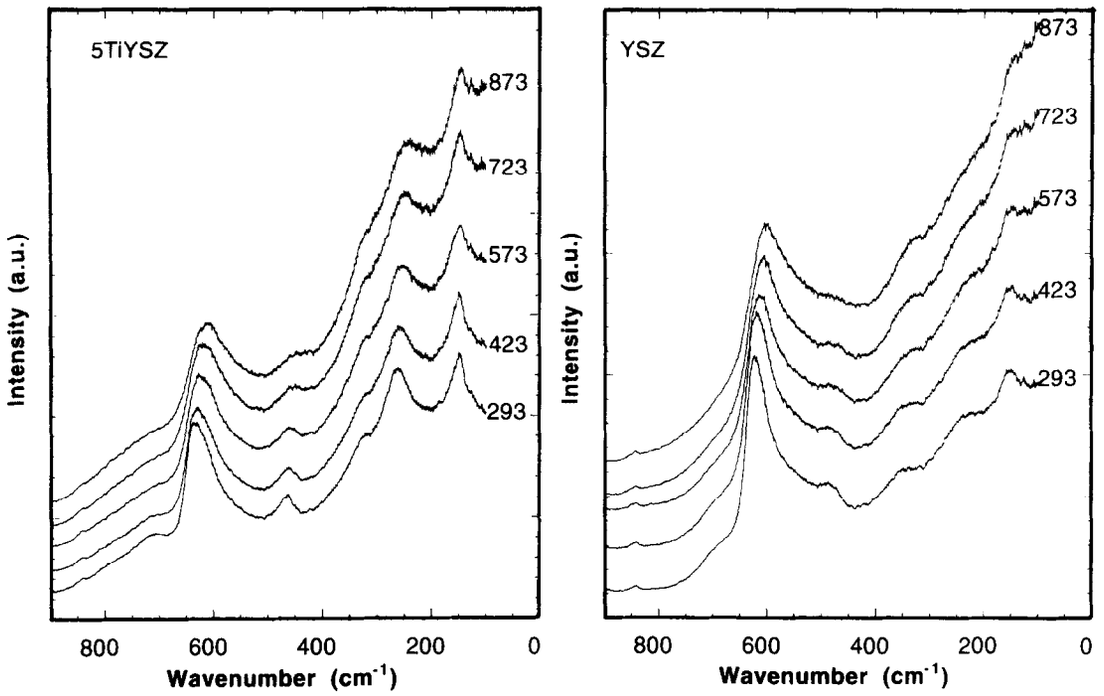

Fig. 6. Raman spectra of 5TiYSZ and YSZ at various temperatures. Labels indicate the temperature in K.

also slightly depressed. Because of the composite nature of 20TiYSZ, and obvious difficulty in analyzing impedance data in terms of grain and grain boundary contributions, preferential attention will be given to the total conductivity of the different materials. Increasing total resistance of the material for increasing titania contents (20TiYSZ versus 1TiYSZ) can be concluded from the Arrhenius plot shown in Fig. 9. In fact, a conductivity drop of over one order of magnitude is observed between composition extremes.

Previously reported data for the bulk conductivity of 10TiYSZ [18] are quite near to those of 20TiYSZ, and well below those of the remaining compositions. Overall differences between 10TiYSZ and 20TiYSZ are not more significant than those observed between 1TiYSZ and 3·5TiYSZ. This trend is already familiar from the literature, where a sharp decrease in conductivity is usually observed between 5TiYSZ and 10TiYSZ.[14,18] Further analysis of data obtained with these materials indicates that the activation energies for ionic migration are similar, and the effect of dopant level is negligible (activation energies below 1073 K: 99·3 kJ mol^{-1} for 1TiYSZ, 98·3 kJ mol^{-1} for 3·5TiYSZ, and 102 kJ mol^{-1} for 20TiYSZ).

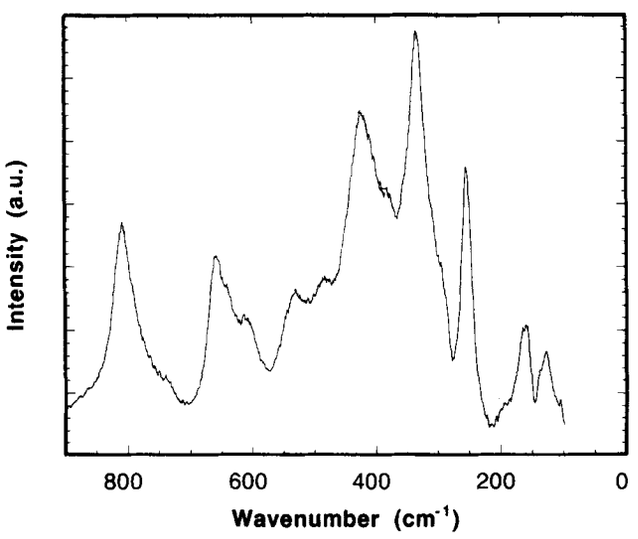

Fig. 7. Difference spectrum obtained by subtracting the 10TiYSZ Raman spectrum from the 20TiYSZ spectrum.

4 Discussion

4.1 Structural effect of titania additions

Present XRD results indicate that a solid solution between titania and cubic YSZ exists up to slightly less than 10 mol% TiO_2. Evidence for the formation of a tetragonal phase is only obtained with the 10TiYSZ sample. For higher titania contents, a zirconium titanate precipitates. X-ray diffraction spectra, which are almost purely dependent on the location of the cations, show a pure cubic structure for low-titania-content materials. However, Raman spectroscopy, which is most sensitive to local order of cation–anion pairs, shows that two local structures are present: cubic and tetragonal. This does not mean that the material is necessarily biphasic, but that there are small domains in which the anion sublattice is fully disordered, as in cubic zirconia, and others in which ordering has occurred. The fact that the difference spectra of Fig. 4 show bands much broader than in the case of tetragonal polycrystalline zirconia

suggests that these ordered domains extend to a small number of nearest neighbours.

An unambiguous explanation on the role of titania in such anion ordering cannot be derived from our experiments. However, as titanium prefers a coordination of 6, we may assume that it traps some oxygen vacancies to move away from the 8 coordination of the Zr site. Li and Chen[3] have proposed a similar explanation for the ability of trivalent cations to stabilize the cubic zirconia structure. From EXAFS and XANES studies, they have shown that trivalent cations smaller than Zr^{4+} trap the oxygen vacancies in order to become sixfold coordinated. As the zirconia stabilization in the cubic structure needs a ratio of sevenfold coordinated to eightfold coordinated zirconium close to one, these small cations stabilize the tetragonal structure of zirconia. We therefore propose that Ti cations trap some oxygen vacancies. For electroneutrality reasons, the number of oxygen vacancies in the vicinity of Zr cations close to a titanium ion will decrease and eightfold coordinated Zr will appear in excess, therefore promoting a tetragonal structure. In this case, the peak at 720 cm^{-1} observed in the Raman spectra could be due to a vibration involving a Ti atom and an oxygen vacancy. As the Raman spectra show that this situation is not changed upon heating, at least up to the highest investigated temperature (873 K), we can assume that the Ti–oxygen vacancy interaction is quite strong. In the other case, a change towards the cubic zirconia spectrum would have been expected.

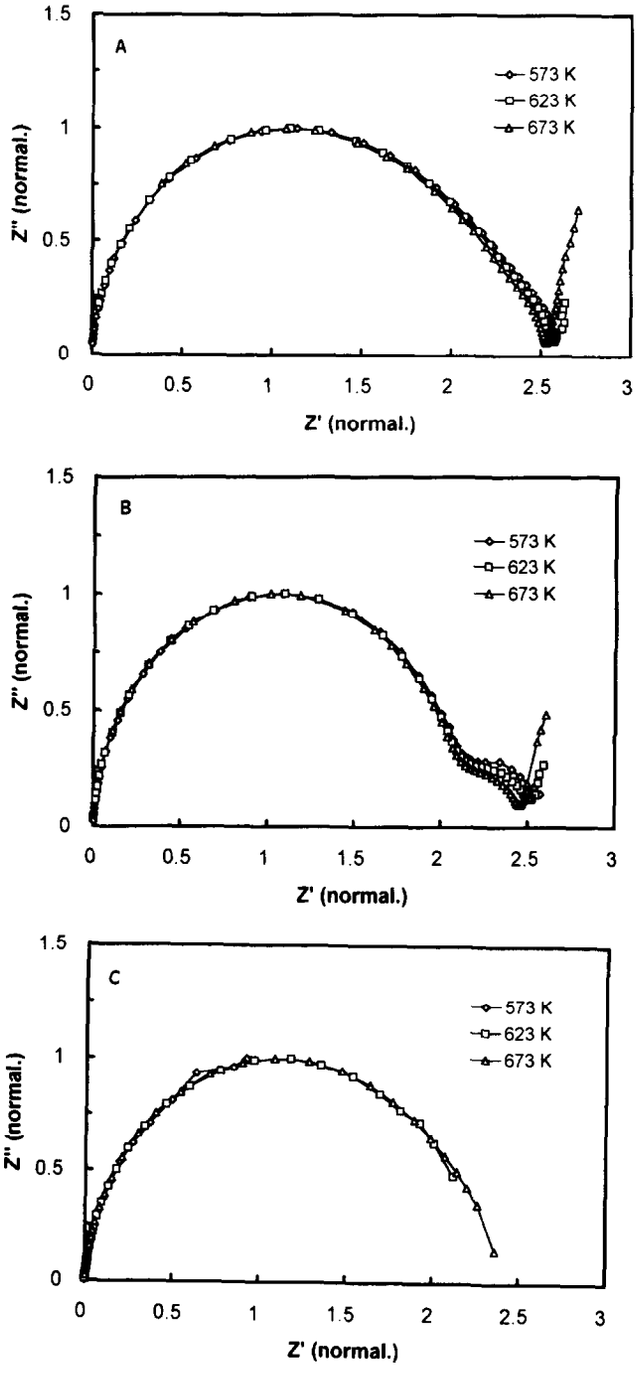

Fig. 8. Impedance spectra of (a) 1TiYSZ, (b) 3·5TiYSZ and (c) 20TiYSZ in air at three different temperatures. The real and imaginary parts of impedance were normalized as described in the text.

4.2 Electrical conductivity

As titanium is a tetravalent dopant, the concentration of oxygen vacancies is still determined by the concentration of yttrium, which means that only a slight overall decrease in concentration of ionic defects should be noticed between undoped and titania-doped YSZ, as a consequence of a simple dilution effect. In fact, the dependence of oxygen vacancy concentration ($[V_O{\cdot\cdot}]_{TiYSZ}$) on titania content can be expressed as a function of titania mole fraction (x / 100) in the doped material:

$$[V_O{\cdot\cdot}]_{TiYSZ} = (100 - x)\,[Y_{Zr}']_{YSZ} / 200 \qquad (1)$$

$[Y_{Zr}']_{YSZ}$ being the concentration of yttrium in zirconium positions in the starting YSZ powder. In this equation the usual Kroger–Vink notation has been used except for an additional subscript indicating the type of material considered (YSZ or titania-doped YSZ). All these aspects suggest that oxygen vacancies are always the dominant mobile

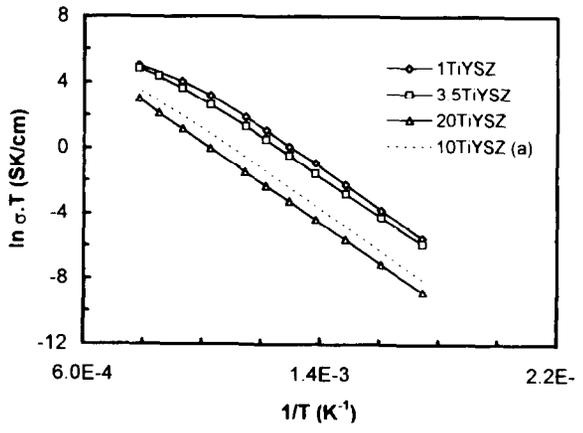

Fig. 9. Arrhenius plot of total conductivity of 1TiYSZ, 3·5TiYSZ, 10TiYSZ and 20TiYSZ. Data for 10TiYSZ from Ref. 18.

defects and that the mechanism for ionic motion is not changed, irrespective of the composition.

The role of dopants in the ionic conductivity usually takes into consideration the effective pathway for oxygen ions moving between consecutive positions. For example, the decrease in ionic conductivity with increasing ceria dopant level is coherent with the estimated decrease in the free radius between the cations through which one oxygen ion must move.[8] Based on the ionic radius of Zr^{4+} and Ce^{4+}, it can be concluded that the substitution of Ce for Zr causes a decrease in this free radius. In fact, the increase in lattice parameter is smaller than the increase in average cation radius. This is expected to cause a decrease in ionic conductivity and increase in activation energy for ionic mobility.[8] This model can explain quite reasonably the effect of some dopants with fluorite or derived structures (ex: C-type cubic). However, when considering the dependence of the free radius for ionic motion on titania content, the result is contradictory to experimental evidence. A significant decrease in ionic conductivity is observed with increasing titania content, but an almost constant activation energy is observed. In this case, the simple effect of the dopant cation radius is not believed to be the dominant parameter.

The central issue is that the dopant induces a different structure. Also for this reason, the solubility limit of titania in YSZ is quite small as compared to other dopants with similar structures (HfO_2, CeO_2, or even Y_2O_3 and rare earth oxides with the C-type cubic structure). We have shown in the previous section that the oxygen sublattice is composed of ordered and disordered regions. A simple explanation would be that oxygen migration occurs mostly in the disordered regions. As the titania content increases, these regions disappear and the electrical conductivity decreases. It is also possible that a percolation phenomenon exaggerates this volume effect. The 10TiYSZ sample could be seen as islands of conductive domains (in which the oxygen sublattice is disordered) in a more insulating matrix (in which the oxygen sublattice is more ordered). Its electrical conductivity would in this case reflect mainly the conductivity of the ordered domains.

As the activation energy for electrical conduction is almost independent of the titania content, one expects that the microscopic process of oxygen migration is unaltered. This is also consistent with the proposed structural model. In yttria-doped zirconia, the anionic disorder is mostly due to the large number of oxygen vacancies. We may think that ordering occurs because oxygen vacancy concentration decreases. Keeping constant the crystalline structure of the material, this would decrease the pre-exponential factor of the electrical conductivity, linked to the number of free charge carriers, and keep constant the activation energy. Raman spectra indicate that increasing the temperature does not change the amount of ordered domains. A constant activation energy is therefore expected.

5 Conclusion

The role of titanium in the electrical behavior of YSZ is believed to be determined mostly by local lattice distortion in the neighborhood of titanium ions, yielding non-equivalent anion sublattice positions. Although XRD macrostructural characterization suggests that most of the compositions are cubic (below 10 mol% TiO_2), Raman spectroscopy has shown that the anion sublattice is composed of tetragonal-like and cubic-like domains having different conductivities mainly because of the lower oxygen vacancy content in the tetragonal-like domains. It is proposed that this decrease in the vacancy concentration is due to the Ti ions, which trap oxygen vacancies to shift from the eightfold coordinated Zr site towards their preferred sixfold coordination. The combination of Raman spectroscopy and impedance spectroscopy has proven to be a useful tool when very local structural changes are involved.

Acknowledgements

The authors are grateful for support from JNICT (Portugal), RG-BPD-228/95, and Dr M. Kleitz who provided the conditions for a visit (F. Marques) to LEPMI-Grenoble. The authors also thank Prof. G. Lucazeau for helpful discussions.

References

1. Kilner, J. A. & Brook, R. J., A study of oxygen ion conductivity in doped non-stoichiometric oxides. *Solid State Ionics*, **6** (1982) 237–252.
2. Kilner, J. A. & Waters, C. D., The effect of dopant cation-oxygen vacancy complexes on the anion transport properties of non-stoichiometric fluorite oxides. *Solid State Ionics*, **6** (1982) 253–259.
3. Li, P. & Chen, I-Wei, Effect of dopants on zirconia-stabilization — An X-ray absorption study: I. Trivalent dopants. *J. Am. Ceram. Soc.*, **77** (1994) 118–128.
4. Li, P. & Chen, I-Wei, Effect of dopants on zirconia-stabilization — An X-ray absorption study: II. Tetravalent dopants. *J. Am. Ceram. Soc.*, **77** (1994) 1281–1288.
5. Li, P. & Chen, I-Wei, Effect of dopants on zirconia-stabilization — An X-ray absorption study: III. Charge compensating dopants. *J. Am. Ceram. Soc.*, **77** (1994) 1289–1295.
6. Calès, B. & Baumard, J. F., Conduction and defect structure of ZrO_2–CeO_2–Y_2O_3 solid solutions, *J. Electrochem. Soc.*, **131** (1983) 2407–2413.

7. Patil, D. S., Ventrakamani, N. & Rohatgi, V. K., Electrical conductivity of $(ZrO_2)_{0.85}$ $(CeO_2)_{0.12}$ $(Y_2O_3)_{0.03}$. *J. Mater. Sci.*, **23** (1988) 3367.
8. Ananthapadmanabhan, P. V., Venkatramani, N., Rohatgi, V. K., Momin, A. C. & Venkateswarlu, K. S., Structure and ionic conductivity of solid solutions in the system $0{\cdot}9\{(ZrO_2)_{1-x} - (CeO_2)_x\} - 0{\cdot}1(Y_2O_3)$. *J. Eur. Ceram. Soc.*, **6** (1990) 111–117.
9. Liou, S. S. & Worrell, W. L., Electrical properties of novel mixed-conducting oxides. *Appl. Physics A*, **49** (1989) 25–31.
10. Liou, S. S. & Worrel, W. L., Mixed conducting oxide electrodes for solid oxide fuel cells. *Proc. 1st Int. Symp. on Solid Oxide Fuel Cells*, ed. S. C. Singhal. The Electrochemical Society, Pennington, 1989, pp. 81–89.
11. Arashi, H. & Naito, H., Oxygen permeability in ZrO_2–TiO_2–Y_2O_3. *Solid State Ionics*, **53–56** (1992) 431–435.
12. Naito, H. & Arashi, H., Electrical properties of ZrO_2–TiO_2–Y_2O_3. *Solid State Ionics*, **53–56** (1992) 436–441.
13. Marques, R. M. C., Frade, J. R. & Marques, F. M. B., Ceramic materials for SOFC anode cermets. *Proc. 3rd Int. Symp. on Solid Oxide Fuel Cells*, ed. S. C. Singhal & H. Iwahara. The Electrochemical Society, Pennington, 1993, pp. 513–522.
14. Colomer, M. T., Jurado, J. R., Marques, R. M. C. & Marques, F. M. B., Evaluation of titania doped YSZ for SOFC anodes. *Proc. 3rd Int. Symp. on Solid Oxide Fuel Cells*, ed. S. C. Singhal & H. Iwahara. The Electrochemical Society, Pennington, 1993, pp. 523–532.
15. Lindegaard, T., Clausen, C. & Mogensen, M., Electrical and electrochemical properties of $Zr_{0.77}Y_{0.13}Ti_{0.1}O_{1.93}$. *Proc. 14th Riso Int. Symp. on Materials Science*, ed. F. W. Poulsen *et al.* Riso National Laboratory, Roskilde, 1993, pp. 311–318.
16. Marques, R. M. C., Marques, F. M. B. & Frade, J. R., Characterization of mixed conductors by dc techniques. Part II: Experimental results. *Solid State Ionics*, **73** (1994) 27–34.
17. Naito, H. & Arashi, H., Thin films fabrication of ZrO_2–TiO_2–Y_2O_3 by laser CVD and their electrical properties. *Solid State Ionics*, **67** (1994) 197–201.
18. Marques, R., Marques, F. & Frade, J., Ionic and electronic conductivity in titania doped YSZ. *Ceramics — Charting the Future, Proc. 8th CIMTEC — World Ceramics Congress, Part D*, ed. P. Vincenzini. Techna SRL, Faenza, 1995, pp. 2625–2632.
19. Colomer, M. T., Traqueia, L. S. M., Jurado, J. R. & Marques, F. M. B., Role of grain boundaries on the electrical properties of titania doped yttria stabilized zirconia. *Mater. Res. Bull.*, **30** (1995) 515–522.
20. Colomer, M. T., Study of electrocatalytic ceramic materials with application in systems for the production of electrical power and/or H_2, O_2, CH_4 and CH_3OH. PhD Thesis, Universidad Autonoma, Madrid, 1995, in Spanish.
21. Tsukuma, K., Transparent titania–yttria–zirconia ceramics. *J. Mater. Science*, **5** (1986) 1143–1144.
22. McHale, A. E. & Roth, R. S., Low temperature phase relationships in the system ZrO_2–TiO_2 *J. Am. Ceram. Soc.*, **69** (1986) 827–832.
23. Cai, J., Raptis, C., Raptis, Y. S. & Anastassakis, E., Temperature dependence of Raman scattering in stabilized cubic zirconia. *Phys. Rev. B*, **51** (1995) 201–209.
24. Kontoyannis, C. G. & Carountzos, G., Quantitative determination of the cubic-to-monoclinic phase transformation in fully stabilized zirconias by Raman spectroscopy. *J. Am. Ceram. Soc.*, **77** (1994) 2191–2194.
25. Hirata, T., Asari, E. & Kitajima, M., Infrared and Raman spectroscopic studies of ZrO_2 polymorphs doped with Y_2O_3 or CeO_2. *J. Solid State Chem.*, **110** (1994) 201–207.
26. Semjonow, A. J. & Anastassakis, E., Asymmetry of defect-induced Raman spectra in yttria-stabilized zirconia. *Physica A*, **201** (1993) 416–420.
27. Ishigame, M. & Yoshida, E., Study of the defect-induced Raman spectra in cubic zirconia. *Solid State Ionics*, **23** (1987) 211–218.
28. Kontoyannis, C. G. & Orkoula, M., Quantitative determination of the cubic, tetragonal and monoclinic phases in partially stabilized zirconias by Raman spectroscopy. *J. Mater. Sci.*, **29** (1994) 5316–5320.
29. Azough, F., Freer, R. & Petzelt, J., A Raman spectral characterization of ceramics in the system ZrO_2–TiO_2. *J. Mater. Sci.*, **28** (1993) 2273–2276.